Radiochim. Acta **99**, 593–599 (2011) / **DOI** 10.1524/ract.2011.1850

Adsorption interaction of astatine species with quartz and gold surfaces

By A. Serov[1,2], N. Aksenov[3], G. Bozhikov[3], R. Eichler[1,2,*], R. Dressler[1], V. Lebedev[3], O. Petrushkin[3], D. Piguet[1], S. Shishkin[3], E. Tereshatov[3], A. Türler[1,2], A. Vögele[1], D. Wittwer[2] and H. W. Gäggeler[1,2]

[1] Laboratory for Radiochemistry and Environmental Chemistry, Paul Scherrer Institute, 5232 Villigen, Switzerland
[2] Departement for Chemistry and Biochemistry, University Bern, 3012 Bern, Switzerland
[3] Flerov Laboratory of Nuclear Reactions, Joint Institute for Nuclear Research, 141980 Dubna, Russia

(Received August 16, 2010; accepted in final form April 8, 2011)

Astatine / Sublimation enthalpy / Adsorption gas chromatography

Summary. The adsorption interaction of various astatine species with quartz and gold surfaces was investigated by gas chromatography methods. Due to variations of the redox potential of the carrier gas elemental astatine, astatine oxide and hypo-astatic acid have been produced. The identification of the astatine compounds is based on the analogy assumption to the gas phase chemistry of the closest homologues in group 17 of the periodic table, iodine and bromine. The deposition temperatures as well as enthalpies of adsorption have been determined for the astatine species. The enhancement of the metallic character within group 17 towards higher Z is clearly confirmed. Macroscopic properties (sublimation enthalpy) of previously unstudied AtO_2 and HAtO were estimated. The determined data for elemental astatine were compared to available literature data. Based on the obtained experimental results possible designs of experiments for studying of chemical properties of the recently discovered element 117 can be suggested.

1. Introduction

Astatine is a radioactive element, which can be found in three natural radioactive decay series. However, only the following short-lived isotopes can be detected: ^{218}At ($T_{1/2}$ = 1.5 s) from the $^{234/238}$U-decay series; ^{215}At ($T_{1/2}$ = 0.1 ms) as well as ^{219}At (most long-lived isotope with $T_{1/2}$ = 56 s) occur in the ^{235}U-decay series. Astatine is claimed to be the rarest naturally-occurring element. The first confirmed discovery of astatine was made in 1940 by Dale R. Corson and co-workers during the irradiation of bismuth with alpha particles [1]. This new element in the periodic table was reported by several researchers as "eka-iodine" and names like alabamine, dakin, helvetium, and anglohelvetium were suggested [2]. The existence of astatine in the uranium-decay series was discovered in 1943 by Karlik and Bernert [3, 4]. The half-life of its longest lived known isotope with the mass number 210 is 8.3 h. This isotope is accessible only by artificial production methods and is well suited to investigate the chemical properties of astatine. It can be produced in complete nuclear fusion reactions or in multi-nucleon transfer reactions accompanying the latter [5, 6]. Nowadays, astatine is attracting attention mainly for two reasons. The first one is based on practical application of some astatine isotopes in radiopharmacy for the treatment of micro-tumors. Several publications are available on this topic and the authors of these works are optimistic to implement the astatine-based cancer-treatment methods in the near future [7, 8]. The second reason to investigate the behavior of astatine is purely fundamental and deals with the chemistry of newly synthesized superheavy elements, *i.e.* elements with $Z > 110$ (SHE), where astatine is a chemical homologue of element E117 in group 17 of the periodic table. So far, the investigation of the chemical properties of these artificial elements was only possible after successful synthesis of relatively long lived isotopes of elements Rf, Db, Sg, Bh, Hs (see for review [9, 10]), Cn, and E114 [11–14]. The elements with atomic numbers Z larger than 112 possess several chemical and physical characteristics making the design of chemical experiments extremely challenging: Half-lives are typically below one second; Production rates are in the order of several atoms per week if recently available heavy ion accelerators are used [15]; Relativistic effects in the electron structure directly affect valence electrons, especially for the SHE [9, 10, 16–18]. All these specialties limit significantly the applicability of chemical methods and techniques to the investigation of the chemical behavior of the SHE. The main approach to final experiments with SHE is based on the investigation of the chemical properties of their lighter homologues in the same groups of the periodic table at the one-atom-at-a-time level. Finally the most suitable experimental conditions have to be selected from the results obtained with the homologues under the assumption that SHE should behave similar. This working principle turned out to be crucial for designing and tuning of experimental set-ups to investigate new elements.

The successful synthesis of the so far missing element with the atomic number 117 was recently reported at the JINR, Dubna, Russia [19]. In preparation of a chemical investigation of element E117, the main goal of the present research was the investigation of the formation of volatile

*Author for correspondence (E-mail: robert.eichler@psi.ch).

astatine species and their adsorption interaction with quartz and gold surfaces. Using the methods of isothermal gas chromatography and thermochromatography the adsorption interactions of different astatine species on quartz and gold surfaces were investigated. The microscopic model of gas solid adsorption chromatography implemented into a Monte Carlo simulation code [20] was used to deduce the standard adsorption enthalpies at zero surface coverage (ΔH_{ads}) of these astatine species on gold and quartz from the experimental observations.

2. Experiment

2.1 Astatine production

2.1.1 ^{201}At production for online experiments

The nuclide ^{201}At ($T_{1/2} = 89.0$ s) was produced in the heavy ion induced nuclear fusion reaction ^{169}Tm(^{40}Ar, $4n$)^{205}Fr ($T_{1/2} = 3.9$ s, α) $\rightarrow$ ^{201}At. The target was prepared by electroplating of Tm_2O_3 with a target thickness of 450 μg cm^{-2} on a Be thin foil backing (12 μm thickness). The target was irradiated with an ^{40}Ar beam with energy of 180 MeV in the center of the target at the PSI PHILIPS cyclotron applying beam intensities between 10^{11}–10^{12} particles per second. From HIVAP calculations [21] applying a code adapted in [22] the production cross sections of francium isotopes in the nuclear fusion reactions of ^{40}Ar and ^{169}Tm were estimated to be in the 1–10 microbarn region (see Fig. 1). The primarily produced ^{205}Fr α-decayed to ^{201}At, which was used for the on-line isothermal gas chromatography experiments (Sect. 2.2).

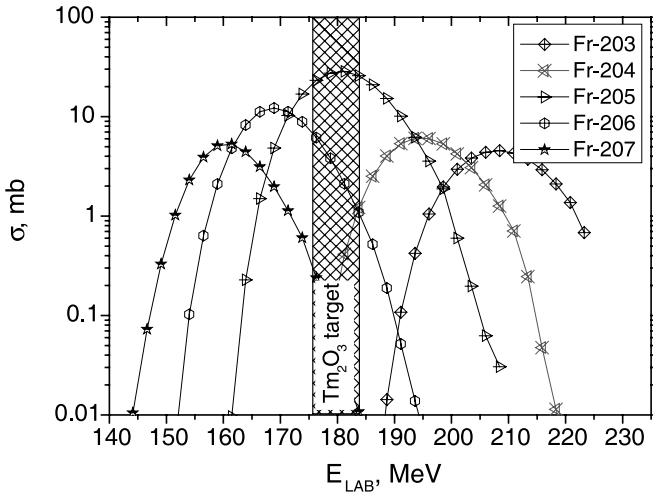

Fig. 1. Production cross-section of different Fr isotopes in the reaction ^{169}Tm(^{40}Ar, xn), calculated with HIVAPSI code [21,22]. The energy range of ^{40}Ar in the target material is indicated.

2.1.2 ^{209}At production for offline experiments

The long-lived ^{209}At ($T_{1/2} = 5.4$ h) was produced in nuclear transfer reactions *via* irradiation of a ^{209}Bi target with ^{40}Ar at the PSI PHILIPS cyclotron. Therefore, a 0.1 mm thick metallic bismuth target was irradiated with ^{40}Ar entering the target with an energy of 220 ± 3 MeV. The products of this reaction were completely stopped in the target. The irradiated Bi samples were introduced into a thermal gas phase separation setup made of quartz (see Fig. 2). The apparatus was flushed with a gas flow of 100 ml min^{-1} of pure He for 20 min to remove the traces of oxygen and water. Afterwards the sample was heated up for 30 min to 1000 °C. The astatine was evaporated and transported by 25 ml min^{-1} pure He into the colder part of the apparatus, where it was deposited on a gold foil. The evaporation time of 30 min was found sufficient for a full separation of astatine from bismuth. The obtained gold foil was used as a source for the off-line thermochromatography experiments (Sect. 2.3).

2.2 Online isothermal chromatographic experiments

The fast online gas phase chemical separation technique – *in-situ* volatilization and online detection system (IVO) as it is described in [11, 23] – was modified to be suitable to perform isothermal gas chromatography experiments with astatine. The schematic experimental setup is depicted in Fig. 3. Heavy ion induced nuclear fusion products recoiling out of the target were thermalized in an argon gas flow. The inner surface of the newly designed recoil chamber of IVO was covered by a quartz insert to prevent any losses of astatine on the chamber walls. Under these conditions only volatile and aerosol-particle bound products were swept out of the recoil chamber through an open quartz column. These products were transported with almost no losses through a Perfluoroalcoxy (PFA®) Teflon™ capillary (1.56 mm inner diameter) at room temperature to a quartz wool filter placed in a quartz tube and heated up by an oven to 850 °C. Aerosol particles produced during beam induced sputtering processes in the target material or in the beam dump were stopped by this filter. Only volatile products such as chlorine and astatine isotopes proceeded further through a 6 m long Teflon™-capillary to a tantalum foil mounted in a quartz tube and heated up to 1000 °C thus acting as a getter for trace amounts of water and oxygen in the carrier gas. Several experiments were performed without this getter to investigate its efficiency. After passing the getter the volatile products entered the chromatography column with an inner diameter

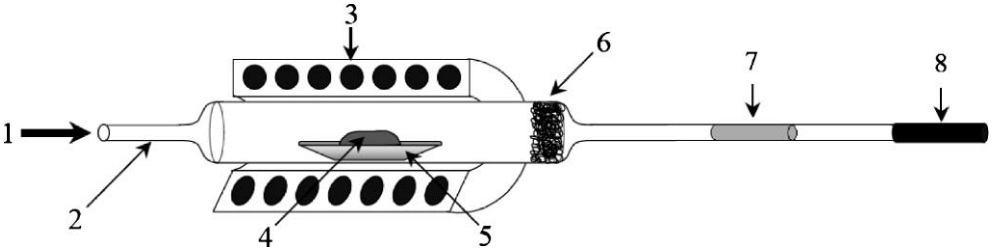

Fig. 2. Experimental set-up used for separation of astatine from the irradiation bismuth target: 1 – carrier gas (He), 2 – quartz column, 3 – volatilization oven (1000 °C), 4 – irradiated bismuth target, 5 – niobium boat, 6 – quartz wool plug, 7 – gold foil, 8 – charcoal trap.

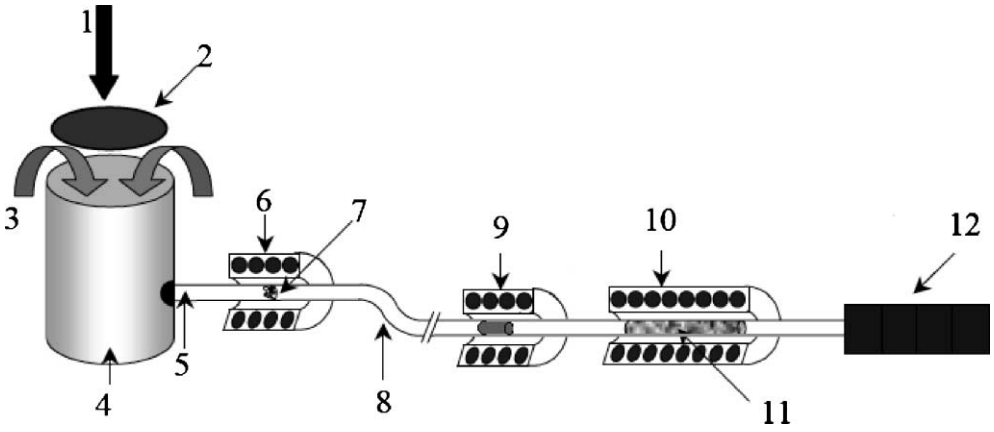

Fig. 3. On-line isothermal gas chromatography set-up: 1 – ^{40}Ar-beam; 2 – Tm_2O_3/Be target; 3 – dried Ar as carrier gas; 4 – recoil chamber lined with quartz; 5 – quartz column; 6 – filter oven (850 °C); 7 – quartz wool plug; 6–8 m PFA capillary; 9 – getter oven with Ta foil (1000 °C); 10 – isothermal oven (IO); 11 – gold; 12 – detection system COLD at room temperature.

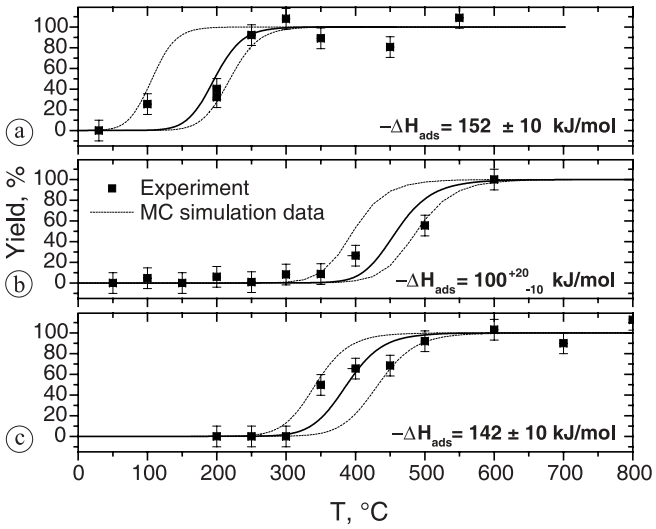

Fig. 4. External chromatograms of ^{201}At adsorption on the stationary gold surface (black squares) together with Monte Carlo simulation data: The solid lines represent the simulations using the best fitting value of the adsorption enthalpy; The thin dashed lines represent the simulations at the upper and lower value of the given error interval of the adsorption enthalpies, respectively. Experimental conditions are: (**a**) argon flow rate 1.8 L min^{-1}, column length – 10 cm, without getter oven; (**b**) argon flow rate 1 L min^{-1}, column length – 10 cm, with getter oven; (**c**) argon flow rate 1 L min^{-1}, column length – 20 cm, with getter oven.

of 4 mm and placed into an isothermal oven (IO). The inner surface of the isothermal part of this column was covered by a gold foil on a length varied between 10 and 20 cm. The astatine, which was able to pass this isothermal part, was further transported through a short PFA capillary to the Cryo On-Line Detector (COLD) [11, 23]. COLD system was modified to contain only 8 pairs of detectors instead of 32. The astatine isotopes passing the isothermal chromatography were deposited on these gold covered detectors held at room temperature and the alpha decay of ^{201}At was registered. Thus, an external chromatogram representing the yield of transported At detected in the COLD in dependence on the temperature of the isothermal column was measured (see Fig. 4). The length of the isothermal stationary gold column used in different experiments is detailed together with all other important experimental parameters such as gas flow and carrier gas treatment in Table 1.

Table 1. Experimental conditions of the isothermal chromatography experiments.

Carrier gas flow rate	Ta-getter in the loop	Temperature ranges (°C)	Column material (length)
A: Ar, 1.8 L min^{-1}	No	650–25	Au (10 cm)
B: Ar, 1 L min^{-1}	Yes	800–200	Au (10 cm)
C: Ar, 1 L min^{-1}	Yes	800–200	Au (20 cm)

2.3 Offline thermochromatographic experiments

The experimental set-up used for the thermochromatography is schematically shown in Fig. 5. The chromatographic column was located inside a hermetically sealed Inconel® steel tube. The carrier gas inlet and outlet were connected by Swagelok® components. Such a system is effective to maintain high carrier gas purities during the experiment by excluding diffusion of oxygen and water into the mobile phase. Additionally, at the beginning of the column a Ta foil was placed acting as a getter for remaining traces of water and oxygen as this zone was heated up to $T = 950$ °C prior to the experiment. The second Ta-getter was located downstream adjacent to the sample at about 980 °C within the temperature gradient to ensure the elemental state of astatine evaporating from the source. The gold foil containing ^{209}At as obtained by the separation procedure from the irradiated bismuth target (described in Sect. 2.1.2) was positioned inside the start oven at the startup of the experiment. After the temperature gradient was established and the getter oven was at 900 °C the start oven was heated up rapidly within about 5 min to $T = 1000$ °C. To investigate the chem-

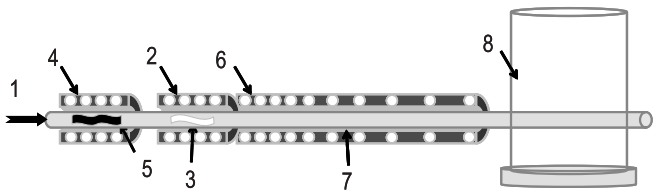

Fig. 5. Offline thermochromatography set-up. 1 – Carrier gas (He, H_2, O_2 or mixtures with water), 2 – starting oven (1000 °C), 3 – ^{209}At source on gold foil surface, 4 – getter oven (1000 °C), 5 – Ta chips, 6 – gradient oven, 7 – chromatographic column (quartz/gold), inner diameter 4 mm, 8 – cooling system (down to liquid nitrogen 77 K temperature).

Table 2. Experimental conditions of thermochromatographic experiments.

Carrier gas	Stationary phase	Flow rate (mL min^{-1})	Experiment duration (min)	Expected species	Species assigned to the observed deposition pattern
H_2	Gold	15	60	At	At
He	Gold	25	60	At	At
He/H_2O^a	Gold	25	60	HAtO	At
O_2	Gold	25	60	AtO,AtO_2	AtO_2
O_2/H_2O^a	Gold	25	60	HAtO	AtO_2
H_2	Quartz	15	60	At	At
He/H_2O^a	Quartz	25	60	HAtO	AtO_2
O_2	Quartz	25	60	AtO, AtO_2	AtO_2
O_2/H_2O^a	Quartz	25	60	HAtO	AtO_2, HAtO

a: Water content was estimated as several volumetric percent.

ical properties of different astatine species in several experiments various carrier gases and carrier gas mixtures were used (see Table 2). In case of oxidizing carrier gases the Ta getters were omitted. The He/H_2O mixture was produced by passing the He gas flow through a water reservoir held at room temperature. Thus, water content can be estimated as several volumetric percents. At the end of the experiment the column was removed from the temperature gradient oven through the cold end. A screening of the activity distribution along the column was performed by a dose meter to roughly identify the position of the astatine activity in the column. Subsequently these positions were measured by gamma spectroscopic measurement using a lead collimator (window size $1 \times 1\,cm^2$, lead thickness 0.7 cm) in front of a standard high purity Ge (HPGe) γ-detector with 2.13 keV resolution at 1.33 MeV in conjunction with an acquisition and analysis system based on Canberra's Genie2k®. All other experimental parameters such as gas flow, stationary phase material, and experiment duration are compiled in Table 2. For the experiments with gold as stationary phase the gradient part of the quartz column was entirely covered inside with rolled gold foils.

3. Results and discussion

3.1 Online isothermal chromatography with gold as stationary phase

It was observed that at high flow rates increasing amounts of astatine passed the gold column already at room temperature and were detected in the COLD. We assume that at these flow rates the aerosol particle filter was not efficient leading to an aerosol particle transport of astatine. Furthermore, it was found that a 10 cm long gold column is too short for depositing all transported astatine on the gold surface at high carrier gas flow rates. The increase of the length of chromatographic column up to 20 cm resulted in a more effective deposition of astatine on the column material. The optimal flow rate was found as 1 L min^{-1}. The results of the isothermal gas chromatography experiments with ^{201}At using gold as stationary phase under three different experimental conditions are shown in Fig. 4a–c together with the Monte Carlo simulation data. Experiments without the tantalum getter revealed the retention of the astatine species at significantly lower temperatures compared to the experiments where the tantalum getter was introduced (Fig. 4a). The most probable explanation is related to the oxidation of astatine by trace amounts of oxygen and water in the carrier gas. This assumption is supported by the observations in the off-line experiments (see Sect. 3.2). Since a speciation of the compound is difficult we refer to it preliminarily as AtO_xH_y. The determined adsorption enthalpy of this species on gold is $-\Delta H_{ads}^{Au}(AtO_xH_y) = 100^{+10}_{-20}$ kJ mol^{-1}.

The series of experiments including efficient removal of the main oxygen and water contaminations by the hot tantalum getter results in an adsorption enthalpy of astatine presumably in its elemental state on gold as $-\Delta H_{ads}^{Au}(At) = 147 \pm 15$ kJ mol^{-1} (Fig. 4b,c).

3.2 Offline thermochromatography

3.2.1 Interaction of astatine species with gold surface

The deposition temperature determined for the astatine species on the gold surface using either purified hydrogen or helium as carrier gas was $T_{dep} = 387 \pm 20$ °C (Fig. 6a,b). Taking into account extremely dry and oxygen free condition in the purified helium and the reduction potential of pure hydrogen this deposition was assigned to astatine in its elemental form. The enthalpy of adsorption of elemental astatine on the gold surface was deduced as $-\Delta H_{ads}^{Au}(At) = 153 \pm 5$ kJ mol^{-1}. This value is within the error bars in good agreement with the data obtained during the online investigation of astatine interaction with gold surface $-\Delta H_{ads}^{Au}(At) = 147 \pm 15$ kJ mol^{-1}. It should be mentioned that despite astatine is supposed to be a halogen no formation of HAt was observed following the trend of decreasing formation enthalpies of the HX (X = F, Cl, Br, I) within group 17. This observation is in good agreement with theoretical calculations predicting low stability of HAt [27]. The non-formation of HAt also explicitly demonstrates the increasing metallic character of the elements within group 17 from fluorine down to astatine. An attempt was performed to form hypoastatic acid (HAtO) using a He/H_2O mixture as carrier gas, as it was described with bromine and iodine in [24]. However, the determined deposition temperature $T_{dep} = 387 \pm 20$ °C indicates that astatine remains in the elemental form at these conditions (see Fig. 6c). The calculated adsorption enthalpy $-\Delta H_{ads}^{Au}(At) = 154 \pm 5$ kJ mol^{-1} is in agreement with the results obtained in the experiments with hydrogen and purified

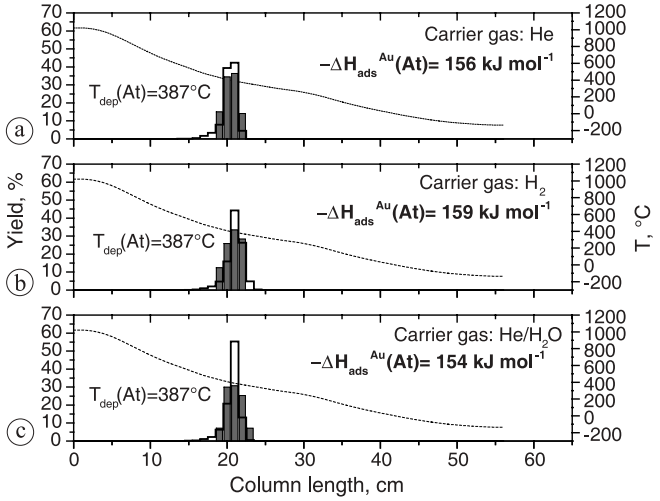

Fig. 6. Thermochromatograms of ^{209}At (dark grey bars, left hand axis) on gold surface using as carrier gas: (**a**) 25 ml min^{-1} He; (**b**) 15 ml min^{-1} H_2; (**c**) 25 ml min^{-1} He/H_2O mixture. The solid stepped lines represent the results of the Monte Carlo simulations applying the adsorption enthalpies given on the panels. The temperature gradients are indicated (dashed line, right hand axis).

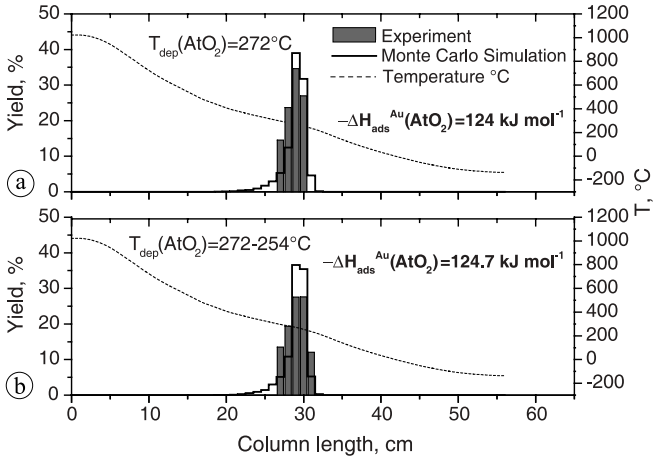

Fig. 7. Thermochromatograms of $^{209}AtO_2$ (grey bars, left hand axis) on gold surface using as carrier gas: (**a**) 25 ml min^{-1} O_2; (**b**) 25 ml min^{-1} O_2/H_2O mixture. The solid stepped lines represent the results of the Monte Carlo simulations applying the adsorption enthalpies given on the panels. The temperature gradients are indicated (dashed line, right hand axis).

helium. This fact indicates the instability of low oxidation states of astatine species at these experimental conditions. The oxidation of astatine and the adsorption of AtO_xH_y on gold surface were studied in pure oxygen as well as in mixed oxygen/water gas atmosphere (Fig. 7a,b). Only one deposited species was observed in both series of experiments with a deposition temperature of $T_{dep} = 272 \pm 20$ °C on gold. The enthalpy of adsorption was calculated as $-\Delta H_{ads}^{Au}(AtO_xH_y) = 124 \pm 5$ kJ mol^{-1}. This value is in good agreement with $-\Delta H_{ads}^{Au}(AtO_xH_y) = 100^{+20}_{-10}$ kJ mol^{-1} obtained in the online experiments with ^{201}At (see Sect. 3.1). Based on a presumed chemical similarity of astatine to the lighter halogen homologues bromine and iodine we tentatively attribute this AtO_xH_y species to the astatine oxide AtO_2, but we cannot exclude that the compound is AtO, which would be a preferred compound for a more metallic element.

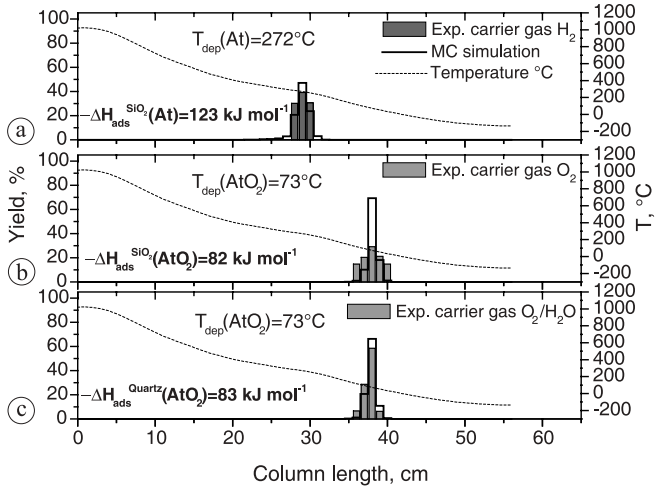

Fig. 8. Thermochromatograms of ^{209}At (dark grey bars, left hand axis) and $^{209}AtO_2$ (grey bars, left hand axis) on quartz surface using as carrier gas: (**a**) 15 ml min^{-1} H_2; (**b**) 25 ml min^{-1} O_2; (**c**) 25 ml min^{-1} O_2/H_2O. The solid stepped lines represent the results of the Monte Carlo simulations applying the adsorption enthalpies given on the panels. The temperature gradients are indicated (dashed line, right hand axis).

3.2.2 Interaction of astatine species with a quartz surface

Using pure hydrogen as carrier gas, astatine in its elemental form was observed to deposit at $T_{dep} = 272 \pm 20$ °C, yielding $-\Delta H_{ads}^{SiO_2}(At) = 123 \pm 10$ kJ mol^{-1} (Fig. 8a). In pure oxygen and O_2/H_2O mixture astatine behaved similar as in the experiments with gold as stationary surface under the same conditions. Only one species was formed and deposited at temperature $T_{dep} = 73 \pm 20$ °C (Fig. 8b,c). From this observation the enthalpy of adsorption was estimated as $-\Delta H_{ads}^{SiO_2}(AtO_2) = 83 \pm 5$ kJ mol^{-1}. However, the behavior of astatine in He/H_2O gas mixture was different from the experiments with gold as stationary surface. On SiO_2, two deposition peaks were located in the thermochromatogram with the following deposition temperatures: $T_{dep}(1) = 63 \pm 20$ °C and $T_{dep}(2) = -79 \pm 20$ °C (Fig. 9). The first depo-

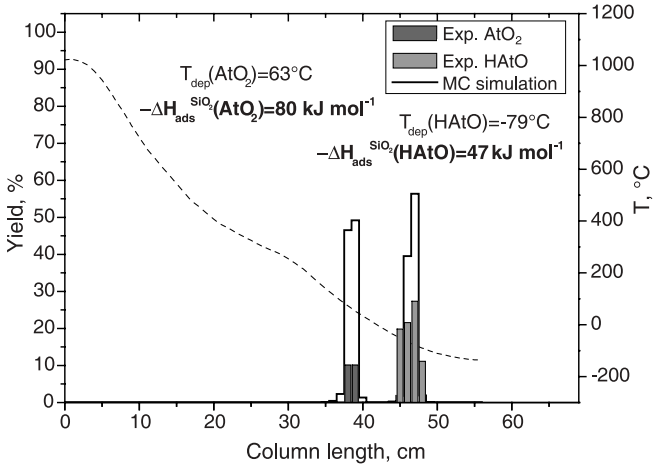

Fig. 9. Thermochromatogram of AtO_2 (gray bars, left hand axis) and HAtO (light grey bars, left hand axis) on quartz surface using as carrier gas 25 ml min^{-1} He/H_2O. The solid stepped lines represent the results of the Monte Carlo simulations applying the adsorption enthalpies given on the panels. The temperature gradient is indicated (dashed line, right hand axis).

sition temperature corresponds to the previously observed AtO_2, whereas the second one we tentatively assign to HAtO. The enthalpies of adsorption were calculated as $-\Delta H_{ads}^{SiO_2}(AtO_2) = 80 \pm 5\,kJ\,mol^{-1}$ and $-\Delta H_{ads}^{SiO_2}(HAtO) = 47 \pm 5\,kJ\,mol^{-1}$. The non formation of HAtO during the experiment under the same condition with gold as stationary surface shows a significant influence of the hydroxo groups on the surface of quartz promoting the formation of hydroxo compounds, especially at lower temperatures.

3.2.3 Validation of presumed speciation

To confirm the elemental state of astatine the correlation plot between sublimation (macroscopic) and adsorption (microscopic) enthalpies for elements on gold surfaces was used (Fig. 10, adapted from [26]). The enthalpy of sublimation for astatine with an corresponding adsorption enthalpy on gold of $-\Delta H_{ads}^{Au}(At) = 153 \pm 5\,kJ\,mol^{-1}$ should be $133 \pm 20\,kJ\,mol^{-1}$, which is larger than $\Delta H_{subl}(At) = 113\,kJ\,mol^{-1}$ reported in [25]. There is another even smaller value of

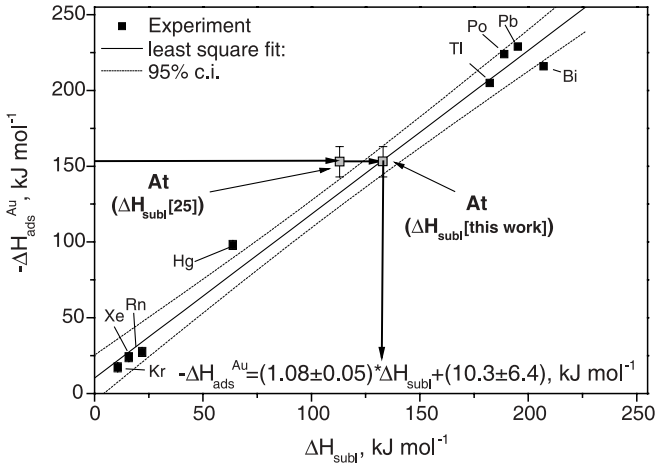

Fig. 10. Correlation of the adsorption enthalpy ΔH_{ads} of the elements on gold surface with their respective macroscopic property of sublimation enthalpy ΔH_{subl} [26]. The value for astatine obtained in this work is shown.

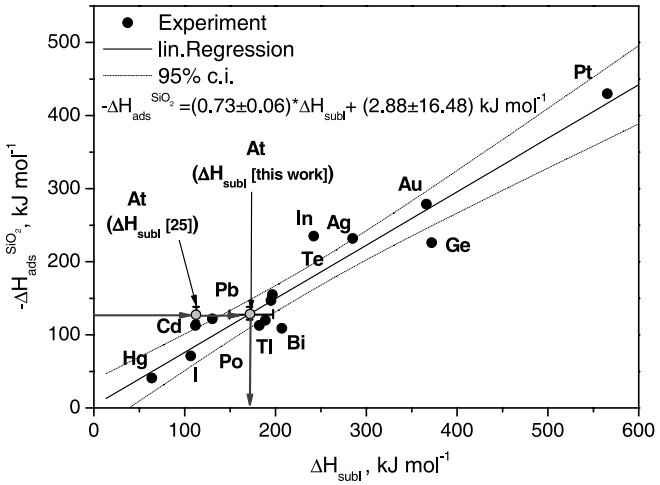

Fig. 11. Correlation of the adsorption enthalpy ΔH_{ads} of the elements on quartz surface with their respective macroscopic property sublimation enthalpy ΔH_{subl} [9]. Value for astatine obtained in this work is shown.

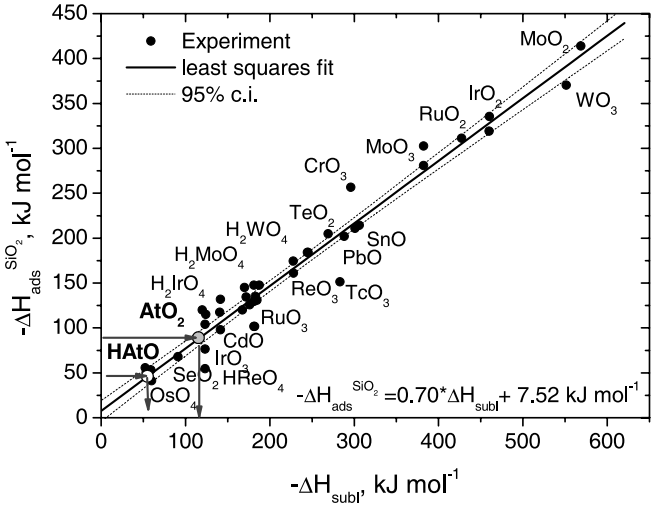

Fig. 12. Correlation of the adsorption enthalpy ΔH_{ads} of oxides and hydroxides on inert surfaces with the macroscopic property of sublimation enthalpy ΔH_{subl} [9]. Values for astatine oxide and hypo-astatic acid obtained in this work are shown.

$-97 \pm 6\,kJ\,mol^{-1}$ given as sublimation enthalpy for astatine in [28].

The correlations between the adsorption enthalpy on quartz and the sublimation enthalpy for elements in their elemental state and for oxides and oxohydroxides adapted from [9] are shown in Figs. 11 and 12, respectively. The sublimation enthalpy deduced from the adsorption enthalpy of astatine on quartz ($-\Delta H_{ads}^{SiO_2}(At) = 124 \pm 5\,kJ\,mol^{-1}$) is $\Delta H_{subl}(At) = 164 \pm 10\,kJ\,mol^{-1}$ which is significantly higher compared to the values given in [25, 28]. We suggest from averaging of our obtained data a new value for the sublimation enthalpy of astatine as $\Delta H_{subl}(At) = 148 \pm 25\,kJ\,mol^{-1}$. From the respective empirical correlation for oxides and oxohydroxides (see Fig. 12) the sublimation enthalpies for AtO_2 and HAtO were estimated for the first time as $\Delta H_{subl}(AtO_2) = 106 \pm 30\,kJ\,mol^{-1}$ and $\Delta H_{subl}(HAtO) = 56 \pm 30\,kJ\,mol^{-1}$, respectively, indicating a higher volatility of these oxidic species of astatine compared to its elemental state.

4. Conclusions

The interaction of astatine species with gold and quartz surfaces was studied by the methods of isothermal gas chromatography and thermochromatography under varied experimental conditions. The tentative speciation suggests elemental astatine, AtO_2 and HAtO formed at varied carrier gas compositions. It was observed that already trace amounts of oxygen and water oxidize “hot” astatine ions recoiling from a heavy ion target. Hence, it can be concluded that the presence of a Ta-getter in the experimental set-ups for the investigation of element 117 E117 in its elemental state might be crucial. The obtained oxidized astatine species are more volatile than elemental astatine and are not strongly interacting with gold. It was also established that astatine in atomic state is less reactive compared to other halogens and forms volatile species such as AtO_2 in contact with both gold and quartz surfaces only under strongly oxidizing conditions, *e.g.* with oxygen being a major com-

ponent of the gas phase. The formation of HAtO was observed only with water being a major component of the gas phase and in contact with quartz surfaces. The experimental results suggest a sublimation enthalpy for astatine as $148 \pm 25\,\mathrm{kJ\,mol^{-1}}$. The sublimation enthalpies for AtO_2 and HAtO were estimated for the first time as $\Delta H_{\mathrm{subl}}(AtO_2) = 106 \pm 30\,\mathrm{kJ\,mol^{-1}}$ and $\Delta H_{\mathrm{subl}}(\mathrm{HAtO}) = 56 \pm 30\,\mathrm{kJ\,mol^{-1}}$, respectively. The formation of HAt was not observed at high temperatures and in pure hydrogen.

The volatility of elements of group 17 (halogens) is decreasing from fluorine to astatine. On the other side metallic character of the elements is increasing. Both trends were confirmed by the present work. These trends suggest a lower volatility of element E117 compared to astatine. The results of these model experiments can serve for the design of an experimental set-up, which is suitable for the investigation of chemical properties of the newest member of the periodic table – element E117.

Acknowledgment. This work was supported by the Swiss National Science Foundation (grant: 200020-117671/1) and by the RFBR (grant No. 09-03-12029-ofi_m).

References

1. Corson, D. R., MacKenzie, K. R., Segrè, E.: Artificially Radioactive Element 85. Phys. Rev. **58**, 672 (1940).
2. Trimble, R. F.: What happened to alabamine, virginium, and illinium? J. Chem. Educ. **52**, 585 (1975).
3. Karlik, B., Bernert, T.: Eine neue natürliche α-Strahlung. Naturwissenschaften **298**(25–26), 31 (1943).
4. Karlik, B., Bernert, T.: Das Element 85 in den natürlichen Zerfallsreihen. Z. Physik **123**(1–2), 51 (1943).
5. Lambrecht, R. M., Mirzadeh, S.: Cyclotron isotopes and radiopharmaceuticals. XXXV: Astatine-211. Int. J. Appl. Radiat. Isot. **36**, 443 (1985).
6. Kuusiniemi, P., Hessberger, F. P., Ackermann, D., Hofmann, S., Kojouharov, I.: Decay studies of $^{210-214}$Fr using alpha-gamma-coincidences. Eur. Phys. J. A **23**, 417 (2005).
7. Zalutsky, M. R., Reardon, D. A., Pozzi, O. R., Vaidyanathan, G., Bigner, D. D.: Targeted α-particle radiotherapy with ^{211}At-labeled monoclonal antibodies. Nucl. Med. Biol. **34**, 779 (2007).
8. Doberenz, I., Doberenz, W., Wunderlich, G., Franke, W.-G., Fisher, S., Dreyer, R., Kessler, L.: Endoarterial therapy of lingual carcinoma using ^{211}At-labelled human serum albumin microspheres: preliminary clinical experience. Nucl. Compact **21**, 124 (1990) [in German].
9. Schädel, M. (ed.): *The Chemistry of Superheavy Elements*. Kluwer Academic Publishers, Dordrecht (2003).
10. Schädel, M.: Chemistry of superheavy elements. Angew. Chem. Int. Ed. **45**, 368 (2006).
11. Eichler, R., Aksenov, N. V., Belozerov, A. V., Bozhikov, G. A., Chepigin, V. I., Dressler, R., Dmitriev, S. N., Gäggeler, H. G., Gorshkov, V. A., Haenssler, F., Itkis, M. G., Lebedev, V. Y., Laube, A., Malyshev, O. N., Oganessian, Yu. Ts., Petruschkin, O. V., Piguet, D., Rasmussen, P., Shishkin, S. V., Shutov, A. V., Svirikhin, A. I., Tereshatov, E. E., Vostokin, G. K., Wegrzecki, M., Yeremin, A. V.: Chemical properties of element 112. Nature **447**, 72–75 (2007).
12. Eichler, R., Aksenov, N. V., Belozerov, A. V., Bozhikov, G. A., Chepigin, V. I., Dressler, R., Dmitriev, S. N., Gäggeler, H. G., Gorshkov, V. A., Haenssler, F., Itkis, M. G., Lebedev, V. Y., Laube, A., Malyshev, O. N., Oganessian, Yu. Ts., Petruschkin, O. V., Piguet, D., Rasmussen, P., Serov, A. A., Shishkin, S. V., Shutov, A. V., Svirikhin, A. I., Tereshatov, E. E., Vostokin, G. K., Wegrzecki, M., Yeremin, A. V.: Thermochemical and physical properties of element 112. Angew. Chem. Int. Ed. **47**(17), 3262 (2008).
13. Wittwer, D., Abdullin, F. Sh., Aksenov, N. V., Albin, Yu. V., Bozhikov, G. A., Dmitriev, S. N., Dressler, R., Eichler, R., Gäggeler, H. W., Henderson, R. A., Hübener, S., Kenneally, J. M., Lebedev, V. Ya., Lobanov, Yu. V., Moody, K. J., Oganessian, Yu. Ts., Petrushkin, O. V., Polyakov, A. N., Piguet, D., Rasmussen, P., Sagaidak, R. N., Serov, A., Shirokovsky, I. V., Shaughnessy, D. A., Shishkin, S. V., Sukhov, A. M., Stoyer, M. A., Stoyer, N. J., Tereshatov, E. E., Tsyganov, Yu. S., Utyonkov, V. K., Vostokin, G. K., Wegrzecki, M., Wilk, P. A.: Gas phase chemical studies of superheavy elements using the Dubna Gas-filled Recoil Separator – stopping range determination. Nucl. Instrum. Methods Phys. Res. B **268**(1), 28 (2010).
14. Eichler, R., Aksenov, N. V., Albin, Yu. V., Belozerov, A. V., Bozhikov, G. A., Chepigin, V. I., Dmitriev, S. N., Dressler, R., Gäggeler, H. W., Gorshkov, V. A., Henderson, R. A., Johnsen, A. M., Kenneally, J. M., Lebedev, V. Ya., Malyshev, O. N., Moody, K. J., Oganessian, Yu. Ts., Petrushkin, O. V., Piguet, D., Popeko, A. G., Rasmussen, P., Serov, A., Shaughnessy, D. A., Shishkin, S. V., Shutov, A. V., Stoyer, M. A., Stoyer, N. J., Svirikhin, A. I., Tereshatov, E. E., Vostokin, G. K., Wegrzecki, M., Wilk, P. A., Wittwer, D., Yeremin, A. V.: Indication for a volatile element 114. Radiochim. Acta **98**, 133 (2010).
15. Oganessian, Yu. Ts.: Heaviest nuclei from ^{48}Ca-induced reactions. J. Phys. G **34**, R165 (2007).
16. Pyykkö, P., Desclaux, J.-P.: Relativity and the periodic system of elements. Acc. Chem. Res. **12**, 276 (1979).
17. Schwerdtfeger, P., Seth, M.: Relativistic effects of the superheavy elements. In: *Encyclopaedia of Computational Chemistry*. Vol. 4, Wiley, New York (1998), p. 2480.
18. Pershina, V.: The chemistry of the superheavy elements and relativistic effects. In: *Relativistic Electronic Structure Theory, Part 2: Applications Theoretical and Computational Chemistry*. Vol. 14 (Schwerdtfeger, P., ed.) Elsevier, Amsterdam (2004).
19. Oganessian, Yu. Ts., Abdullin, F. Sh., Bailey, P. D., Benker, D. E., Bennett, M. E., Dmitriev, S. N., Ezold, J. G., Hamilton, J. H., Henderson, R. A., Itkis, M. G., Lobanov, Yu.V., Mezentsev, A. N., Moody, K. J., Nelson, S. L., Polyakov, A. N., Porter, C. E., Ramayya, A. V., Riley, F. D., Roberto, J. B., Ryabinin, M. A., Rykaczewski, K. P., Sagaidak, R. N., Shaughnessy, D. A., Shirokovsky, I. V., Stoyer, M. A., Subbotin, V. G., Sudowe, R., Sukhov, A. M., Tsyganov, Yu. S., Utyonkov, V. K., Voinov, A. A., Vostokin, G. K., Wilk, P. A.: Synthesis of a new element with atomic number $Z = 117$. Phys. Rev. Lett. **104**, 142502 (2010).
20. Zvara, I.: Simulation of thermochromatographic processes by the Monte Carlo method. Radiochim. Acta **38**, 95 (1985).
21. Reisdorf, W., Schädel, M.: How well do we understand the synthesis of heavy elements by heavy-ion induced fusion? Z. Phys. A **343**, 47 (1992).
22. Dressler, R.: HIVAPSI. A Program to estimate cross-sections in heavy Ion reactions Paul Scherrer Institut (PSI) Scientific Report Vol. I (1999), p. 131.
23. Soverna, S., Dressler, R., Düllmann, Ch. E., Eichler, B., Eichler, R., Gäggeler, H. W., Haenssler, F., Niklaus, J.-P., Piguet, D., Qin, Z., Türler, A., Yakushev, A. B.: Thermochromatographic studies of mercury and radon on transition metal surfaces. Radiochim. Acta **93**, 1 (2005).
24. Wachsmuth, M., Eichler, B., Tobler, L., Jost, D. T., Gäggeler, H. W., Ammann, M.: On-line gas-phase separation of short-lived bromine nuclides from precursor selenium. Radiochim. Acta **88**, 873 (2000).
25. Scientific Group Thermodata Europe (SGTE): Thermodynamic Properties of Elements, Ac to C60. SpringerMaterials – The Landolt–Börnstein Database (http://www.springermaterials.com), doi: 10.1007/10652891_4.
26. Eichler, R.: Empirical relation between the adsorption properties of elements on gold surfaces and their volatility. Radiochim. Acta **93**, 245 (2005).
27. Visscher, L., Styszyñski, J., Nieuwpoort, W. C.: Relativistic and correlation effects on molecular properties. II. The hydrogen halides HF, HCl, HBr, HI, and HAt. J. Chem. Phys. **105**(5), 1 (1996).
28. Online database "Thermo-constants for elements and substances", http://www.chem.msu.su/cgi-bin/tkv.pl?show=welcome.html [in Russian].